

## A Dynamic Modeling Capability for Subcritical Vapor Compression Refrigeration System

Dr. Jafar M. Hassan\*, Dr. Ali H. Tarrad\*\*  
& Dr. Mohammed N. Abdullah\*\*\*

Received on: 4/3/2009

Accepted on:2/7/2009

### Abstract

In this investigation the individual component models for a typical subcritical cycle are developed based on the best published theoretical and empirical literature. The developed approach, especially for air conditioning systems, is conceptually new and can be used with modification to a variety of multi-component system applications. The component models are then integrated and the model predictions validated against the data from various experimental test systems.

A variable speed compressor test rig was used to obtain the experimental data to be compared with the results predicted from the system model. The experimental data was monitored from the start-up of the system until the achievement of its steady-state. The system approached its steady-state after 270 sec and 360 sec for compressor speeds of 900 rpm and 1200 rpm respectively. The system disturbance was imposed by changing the operation conditions for each component. A comparison between the experimental data for these disturbances and theoretical results shows a good agreement with a discrepancy of about (5%). The model can be used as a basis for the design, performance and efficiency of a vapor compression systems.

**Keywords:** Transient, Modeling, Subcritical, Multi-component, Compression Systems.

### تطوير نموذج ديناميكي لدورة البخار اللانضغاطية لمنظومات التثليج

#### الخلاصة

في هذا البحث تم إعداد النموذج الرياضي لكل معدة من دورة التثليج الانضغاطية استنادا الى أفضل النشريات من البحوث النظرية والتجريبية وخاصة بالنسبة لمنظومات تكييف الهواء. ويمكن استخدام هذه النماذج مع بعض التعديلات في المنظومات متعددة المكونات. وتم تجميع النماذج الرياضية لكل معدة في نموذج رياضي متكامل وتم مقارنة النتائج النظرية مع نتائج التجارب العملية. تم استخدام منظومة تثليج ذات ضاغطة متغيرة السرعة لغرض الحصول على القراءات العملية ومقارنتها مع النتائج المستحصلة من النموذج الرياضي. أخذت القراءات عند تشغيل المنظومة لغاية حصول حالة الاستقرار للمنظومة ، حيث أجريت التجارب عند سرعة الضاغطة 900 دورة/دقيقة وجد إن الزمن اللازم لحصول حالة الاستقرار 270 ثانية ، بينما الزمن اللازم لحصول حالة الاستقرار 360 ثانية عند سرعة الضاغطة 1200 دورة/دقيقة . بعد ذلك تم تغيير ظروف التشغيل لكل معدة على حدة مع الإبقاء على الظروف التشغيلية لباقي المعدات دون تغيير، وتمت مقارنة النتائج العملية والنظرية حيث لوحظ هناك توافق جيد وبنسبة خطأ 5% . إن النموذج الرياضي يمكن استخدامه في تصميم وتحديد معامل الأداء وكفاءة منظومة التثليج الانضغاطية.

\* Mechanical Engineering Department, University of Technology / Baghdad

\*\* Mechanical Engineering Department, College of Engineering, Al-Mustansiriyah University / Baghdad

\*\*\* Ministry of Industry and Minerals / Baghdad

### Introduction

Refrigeration systems are widely used and can be found in various places such as building for air conditioning, supermarkets, automotives, etc. These systems in principle all work in the same way, they utilize a vapor compression (VC) cycle process to transfer heat. A brief introduction to the most common thermodynamical properties and relations for the VC cycle is cited in [1], (2005).

During the last few years many publications related to the dynamic modeling of heat pumps, refrigerators, evaporators, and condensers. These can be classified into four categories: black box models, one-zone models, two-zone models, and distributed models..

MacArthur and Grald (1988) [2] presented a cyclic VC heat pump performance with a fully distributed model. A detailed mathematical treatment is given for the evaporator and condenser. Lumped-parameter models are developed for expansion valve and compressor. Inclusion of an appropriate void fraction model is found to be essential in determining the detailed refrigerant mass distribution, this topic is also discussed. Simulation results and experimental data are compared with the transient operation of a hermetic water to water heat pump and air to air system with an open compressor.

Sean, and Curt (1993)[3], developed semi-theoretical steady

state and transient models of a mobile A/C evaporator for use in a complete system simulation. The steady state evaporator heat transfer model is a simplification of the enthalpy potential model presented in the ASHRAE Equipment Handbook and correlated the measured data within 5%.

Atear et. al. (1995) [4] developed three different approaches for the prediction of transient performance of cross-flow finned tube, liquid/gas heat exchangers. The temperature variation of both fluids between inlet and exit is assumed to be linear, and the effective rate of the heat transfer is assumed to be proportional to the difference of the average temperature on both sides.

James Solberg et. al. (2000)[5] studied the traditional method of controlling evaporator superheat in VC air conditioning system that is Thermostatic Expansion Valve (TXV). A new sensor was presented that can sense refrigerant with low mass flow rate. The dynamics of the sensor allow it to detect saturated liquid droplets in superheated vapor.

Xuquan et. al. (2004)[6] described the improvement of refrigerant flow control method by using an Electronic Expansion Valve (EEV) which is driven by a stepper motor in automobile A/C system. An EEV can make a quick response to the abrupt change in automobile speed and the TXV

on/off operation.

Xia et al. (2004)[7], presented a testing methodology applicable to variable refrigerant flow (VRF) equipment. They used two compressors, one runs at variable speed, and other runs at constant speed. They found that actual compressor performance is compared to the ideal isentropic process with the same inlet pressure and temperature and the same outlet pressure.

Tarrad and Shehhab (2007)[8], investigated the performance of an air conditioning unit during the steady state conditions. Theoretical and experimental studies were conducted to simulate the COP of a vapor compression refrigeration cycle, using R-22 as circulating refrigerant. The experiments showed a rapid response of the cooling unit performance to any variation of the environment conditions. Increasing of the entering air temperature to the cooling coil of the refrigeration unit revealed a decrease in the COP of cycle.

In this paper a dynamic modeling capability for vapor compression system is developed.

The modeling methodology is developed with the multiple objectives of predicting control and design.

#### **Experimental Work:**

The test rig layout is shown schematically in Figure (1), and photographically in Figure (2) and Figure (3). It consists of a refrigeration unit, water circulation system and measuring instrumentation.

The refrigeration unit is essentially a laboratory G. Cusson

refrigeration unit made by G. Cusson Co. (England), model P5750. It uses a simple VC cycle with R-12 as working fluid. Many modifications were made to meet the requirements of this study concerning the transient response of the refrigeration system.

The test is standard including measuring of, temperature at eight locations at the same time, as well as the pressure at compressor suction and discharge, and expansion valve pressure through the computer software. The torque and speed are measured directly from the panel. The test is finished when the steady-state has been achieved. To simulate the operation with the dynamic refrigerator model, a preliminary run has been made from initial conditions.

The test was commenced when the steady state conditions has been disturbed by changing the expansion valve opening, compressor speed, water flow rate passing through condenser and water flow rate passing through evaporator.

Table (1) represents the detailed geometry features of the major parts of the cooling system.

#### **First Principle Model:**

Mathematical models of different components of a vapor compression cycle are presented. The operation of such a typical system can be divided primarily into two time regimes, namely steady-state and transient. In steady-state, the system input-output parameters are constant over time, whereas transient response can be analyzed in the presence of time varying inputs,

disturbances acting on the system. The cause of these disturbances sensible and latent capacity. Efficiency depends on the state of refrigerant at evaporator outlet (i.e. Superheat degree). A unit with no superheat would be ideal because heat transfer efficiency reduces as superheat increases. However, a minimum positive superheat is essential to avoid liquid carryover that could damage the compressor [9]. Sensible and latent capacities are affected by modulating the evaporator water and refrigerant mass flow rates.

Finite difference techniques and Lumped Parameter methods are the two primary approaches for the physics-based modeling of vapor compression systems. Finite difference methods have been successfully used by references [10,11] for simulation work. However, a very high-order system representation is obtained by these methods which is not conducive to the design of advanced controllers. On the other hand, Lumped Parameter methods generate relatively low order models which are preferred for controls perspective. Development of this method can be recognized to the work by Wedekind et al. [12] on generalized mean void fraction models for heat exchangers. Various works [10,13] have been done based on that idea, and the same approach will be used in this study too.

Dynamic model for a complex system is preferably obtained by modeling each of its individual components and integrating them together. Design of component models requires knowledge of

complete underlying physics of the system and the integration step is also facilitated by that knowledge. For subcritical vapor compression cycles, the four primary components are the evaporator, the condenser, the expansion valve and the compressor as shown in Figure(1). Nonlinear models for the evaporator, the expansion valve and the compressor, and condenser using the approach of PDE method, which requires knowledge of underlying physics., and the moving boundary approach, was used for heat exchanger modeling is followed in this method [13, 14]. In industrial systems, a receiver or an accumulator [15] is usually used with the heat exchangers in order to improve the system's operation efficiency as well as to avoid damage to the compressor.

#### **Dynamic Model of a Condenser:**

A subcritical system condenser is a higher pressure side heat exchanger through which the refrigerant loses energy to the external fluid, usually water or air. Typical industrially available condensers have varied designs and geometries [16], like, shell and tube, plate-fin etc. Numerical techniques and computational fluid dynamics methods have been extensively used for modeling of these systems [17].

#### **Modes of Operation:**

A subcritical vapor compression system condenser can operate in three different conditions, which in turn decides the number of different fluid regions, it accommodates [9]. The inlet condition to the condenser is always assumed to be superheated vapor and the most typical

operational condition occurs when the fluid at the condenser outlet is subcooled. Thus, the condenser has three different fluid regions, superheated, two phase, and subcooled, namely, as shown in Figure (4). In such a flow condition, the lengths of different regions form important dynamic variables of interest.

**PDE Method for Condenser Modeling:**

Generalized Navier-Stokes equations [18] can be used to express mass and energy conservation for the three different fluid flow regions for the condenser shown in Figure (4). The governing Newtonian PDEs for the three regions are given by;

**Refrigerant mass balance:**

$$\frac{\partial r}{\partial t} + \frac{\partial(ru)}{\partial z} = 0 \quad \dots(1)$$

**Refrigerant energy balance:**

$$\frac{\partial(rh - P)}{\partial t} + \frac{\partial(ruh)}{\partial z} = \frac{4}{D_i} a_i (T_w - T_r) \dots(2)$$

**Condenser Wall energy balance:**

$$(rAC_p) \frac{\partial(T_w)}{\partial t} = a_i p_i (T_r - T_w) + a_o p_o (T_{wu} - T_w) \dots(3)$$

**Simplification of the PDEs:**

The governing PDEs presented are used to derive lumped parameter ODEs to model the dynamics of two-phase flow heat exchangers. These equations are integrated along the length of the tube for each section of tube. To perform the necessary integrations, an integration rule commonly known as Leibniz's equation will be used (equation 4), with z or x being spatial coordinates. Thus, the limits

of integration depend on how the regions are defined for each heat exchanger[3].

$$\int_{z_1(t)}^{z_2(t)} \frac{\partial f(z,t)}{\partial t} dz = \frac{d}{dt} \left[ \int_{z_1(t)}^{z_2(t)} f(z,t) dz \right] - f(z_2(t),t) \frac{d(z_2(t))}{dt} + f(z_1(t),t) \frac{d(z_1(t))}{dt} \dots(4)$$

The resulting ordinary differential equations can be combined, and simplified to be fed to the Simulink Simulation package. The resulting set of equations can be solved numerically given appropriate initial boundary conditions.

**Refrigerant Mass Conservation: Superheat Region:**

After multiplying the Navier-Stokes relation by cross sectional area and eliminating the y component of the Equation (1), the PDE for conservation of the refrigerant mass is given by,

$$\frac{\partial rA}{\partial t} + \frac{\partial(ru)}{\partial z} = 0 \quad \dots(5)$$

By integrating each term of Equation (5) over the length of the superheated region (say, L=0 to L=L1). Applying Leibniz's rule and assuming that  $r = r(P, h)$  and  $h = (h_i + h_o)/2$ .

Thus, the mass conservation equation in the superheated region is given by;

$$\left( \frac{\partial r_1}{\partial P} + \frac{1}{2} \frac{\partial r_1}{\partial h_1} \frac{\partial h_g}{\partial P} \right) A L_1 \dot{m}_1 + \left( \frac{1}{2} \frac{\partial r_1}{\partial h_1} \right) A L_1 \dot{h}_i \dots(6)$$

$$+ (r_1 - r_g) A L_1 \dot{m}_1 - \dot{m}_1 = 0$$

**Two Phase Region:**

The same PDE for mass conservation given by Equation (5)

can be used for this region too. The resulting complete equation for mass conservation is given by [9, 22];

$$A \left[ (r_g - r_f) \rho_2 + \left( \frac{dr_f}{dP} (1-g) + \frac{dr_g}{dP} g \right) \rho_2 \right] + \dot{m}_{int2} - \dot{m}_{int1} = 0 \quad \dots(7)$$

**Subcooled Region:**

The PDE for mass conservation is again represented by Equation (5) over the subcooled flow condition. Integrating the equation over the length of the subcooled region,

$$\left( \frac{\partial r_3}{\partial P} + \frac{1}{2} \frac{\partial r_3}{\partial h_3} \frac{\partial h_f}{\partial P} \right) AL_3 \rho + \frac{1}{2} \frac{\partial r_3}{\partial h_3} AL_3 \rho_o + A(r_f - r_3)(\rho_1 + \rho_2) + \dot{m}_o - \dot{m}_{int2} = 0 \quad \dots(8)$$

**Refrigerant Energy Conservation: Superheat Region:**

The dynamics for the conservation of refrigerant energy in any internal flow condition can be represented by the Navier-Stokes law given by,

$$\frac{\partial(rAh - AP)}{\partial t} + \frac{\partial(\dot{m}h)}{\partial z} = p_i a_i (T_w - T_r) \quad \dots(9)$$

By following the method of removal of spatial dependence through energy balance equations in each of the fluid flow regions by integrating over the length of superheated region and applying Leibniz's rule, The energy conservation equation becomes,

$$\left[ \left( \frac{\partial r_1}{\partial P} + \frac{1}{2} \frac{\partial r_1}{\partial h_1} \frac{dh_g}{dP} \right) \rho_1 + \frac{1}{2} \frac{dh_g}{dP} r_1 - 1 \right] AL_1 \rho + \left[ \left( \frac{1}{2} \frac{\partial r_1}{\partial h_1} \right) \rho_1 + \frac{1}{2} r_1 \right] AL_1 \rho_o + (r_1 h_1 - r_g h_g) A \rho_1 + \dot{m}_{int1} h_g - \dot{m}_i h_i = a_{i1} A_i \frac{L_1}{L_{total}} (T_{w1} - T_{r1}) \quad \dots(10)$$

**Two Phase Region:**

For the two phase flow region, the resulting conservation of energy equation can be written as,

$$A \left[ \left( r_g h_g - r_f h_f \right) \rho_1 + \left( r_g h_g - r_f h_f \right) \rho_2 + \left[ \left( \frac{d(r_f h_f)}{dP} (1-g) + \frac{d(r_g h_g)}{dP} g \right) L_2 \rho + (r_g h_g - r_f h_f) \rho_2 \right] - AL_2 \rho + \dot{m}_{int2} h_f - \dot{m}_{int1} h_g = a_{i2} A_i \left( \frac{L_2}{L_{total}} \right) (T_{w2} - T_{r2}) \quad \dots(11)$$

**Subcooled Region:**

The conservation of subcooled region energy can be written as,

$$A \left[ \frac{1}{2} r_3 L_3 \left( \rho_o + \frac{\partial h_f}{\partial P} \rho \right) + \left[ \frac{\partial r_3}{\partial P} \rho + \frac{\partial r_3}{\partial h_3} \left( \frac{1}{2} \left( \frac{\partial h_f}{\partial P} \rho + \rho_o \right) \right) \right] \right] - AL_3 \rho + \left[ h_3 L_3 + (r_f h_f - r_3 h_3) \right] (\rho_1 + \rho_2) + \dot{m}_o h_o - \dot{m}_{int2} h_f = a_{i3} A_i \frac{L_3}{L_{total}} (T_{w3} - T_{r3}) \quad \dots(12)$$

**Pipe Wall Energy Conservation:**

For one dimensional conduction through the tube wall, the wall temperature can be assumed to be uniform over each fluid flow region. The wall temperature gradient depends on incoming and outgoing heat flux represented by,

$$m_w C_{p,w} \frac{\partial T_w}{\partial t} = a_{i1} A_i (T_{r1} - T_{w1}) + a_o A_o (T_{w1} - T_{w1}) \quad \dots(13)$$

The water temperature flowing on the heat exchanger can be assumed to be constant over the length of heat exchanger and can be calculated as the average of the inlet and the outlet water temperatures. Integrating Equation (14) over an arbitrary length of the wall tube,

$$\int_{z_1}^{z_2} m_w C_{p,w} \frac{\partial T_w}{\partial t} dz = \int_{z_1}^{z_2} \left( a_{i1} A_i (T_{r1} - T_{w1}) + a_o A_o (T_{w1} - T_{w1}) \right) dz \quad \dots(14)$$

Applying Leibniz's rule for integration, getting

$$m_w C_{p,w} \left[ (z_2 - z_1) \frac{dT_w}{dt} + [T_w|_{z_1} - T_w|_{z_2-z_1}] \frac{dz_1}{dt} - [T_w|_{z_2} - T_w|_{z_2-z_1}] \frac{dz_2}{dt} \right] = (a_{i1} A_i (T_{r1} - T_{w1}) + a_o A_o (T_{wa} - T_{w1})) (z_2 - z_1) \dots(15)$$

Since the heat transfer behavior of the external fluid (air, water etc.) is considered uniform over the complete wall length, Equation (15) can be used for conservation of wall energy in all the three regions of fluid flow. For superheated region, the limits of integration change to (0 to L1) and the equation can be expressed as,

$$m_w C_{p,w} \left[ L_1 \frac{dT_{w1}}{dt} - [T_{w2} - T_{w1}] \frac{dL_1}{dt} \right] = (a_{i1} A_i (T_{r1} - T_{w1}) + a_o A_o (T_{wa} - T_{w1})) L_1 \dots(16)$$

Similarly, for the other two regions, the wall energy balance is represented by,

$$m_w C_{p,w} \left[ L_1 \frac{dT_{w2}}{dt} \right] = (a_{i2} A_i (T_{r2} - T_{w2}) + a_o A_o (T_{wa} - T_{w2})) L_2 \dots(17)$$

and,

$$m_w C_{p,w} \left[ L_3 \frac{dT_{w3}}{dt} - [T_{w3} - T_{w2}] \frac{d(L_1 + L_2)}{dt} \right] = (a_{i2} A_i (T_{r3} - T_{w3}) + a_o A_o (T_{wa} - T_{w3})) L_3 \dots(18)$$

**Evaporator**

The evaporator is assumed to operate in one of three different conditions: with one, two, or three fluid regions. Note that the same assumptions apply to the condenser, but with the order of the regions reversed.

The detailed derivation of the mass conservation equations, energy conservation equations, and

conservation of wall tube energy equations are found in [9] and [19].

**Modeling for Expansion Valves with Variable Cv:**

As described in [9], the time constant for the dominant dynamics in valve and compressor is much faster than that in the heat exchangers, which implies that static equations can be used for these two components.

For valve modeling, an orifice equation will be used, such that mass flow rate depends on area of orifice opening and pressure gradient between the inlet and the outlet of the valve, and the density at the inlet port. The equation for the orifice model is given by,

$$\dot{m} = C_v A_v \sqrt{\rho \Delta P} \dots(19)$$

In commercial as well as domestic applications of these orifice type metering devices, the mass flow rates change over a wide range during operation cycle. Figure (5) shows a commercially available Hoke metering valve (model number 1315G4B) [20], and its coefficient of discharge characteristics are presented in the figure too with respect to change in the opening area. Stearns [21] suggested that choice of a proper value for coefficient of discharge Cv depends on the evaluation of the flow Reynolds number, which in turn depends on the flow rate. For a given flow condition, the Reynolds number is given by,

$$Re_d = \frac{4 \dot{m}}{\rho d m} \dots(20)$$

According to [21], a simple correlation can be used for the calculation of a dynamic or variable coefficient of discharge which can be represented by,

$$C_v = C_\infty \left( 1 + \frac{C_1}{Re_d} \right) \quad \dots(21)$$

This correlation is known as inv Reynolds [21]. Here,  $C_\infty$  is the coefficient of discharge for infinite Reynolds number (i.e. the minimum value of  $C_v$ ) for a particular orifice and the pipe size. For the system design, it is obtained on the basis of pipe size and diameter ratio.

#### **System Simulation and Discussion:**

The VC system simulation was done for transient response in two modes of operation as following:-

##### **Start-Up Transient Response:**

Start-up transient response for each component of the system until the system achieved its steady state (i.e. the mass flow rate through compressor is equal to the mass flow rate through the expansion valve ). A computer program was written in FORTRAN to calculate the physical properties of refrigerant at each state point as well as the pressure and temperature. The cooling capacity, heat rejected, compressor work, and COP of system and for the cycle were calculated also. The program consists of many subroutines for calculating the saturation pressure and temperature, as well as calculating the compressor volumetric efficiency. The initial conditions can be set to the saturated refrigerant vapor in the heat exchangers at pressure equal to the saturation pressure at the surrounding water temperature. The boundary conditions applied are the refrigerant conditions at the tube coil and water conditions onto the heat exchangers coil. For refrigerant, the inlet boundary

conditions for the condenser, are the compressor mass flow rate and the discharge enthalpy, whereas the exit boundary condition is the expansion valve mass flow rate. For the evaporator, the inlet boundary conditions, are the expansion valve mass flow rate and the enthalpy leaving the condenser ( since the expansion process is isenthalpic), whereas the outlet boundary condition is the mass flow rate into compressor.

The parameters, to be discussed here, are the system pressure, temperature, mass flows and energy flows. Initially, the temperature of the condenser and evaporator wall , the water and the refrigerant in the coils is 26 oC. At this temperature, the condenser and evaporator are both at the equilibrium saturation pressure at 6.7 bar. In the first test, the water flow rate and water entering temperature to condenser and evaporator are constant at 0.0314 kg/sec (25 GPH) and 26 oC respectively. The compressor speed is constant at 900 rpm.

Figure (6) shows the mass flow rate through the compressor as well as the flow rate through the expansion valve. The refrigerant mass flow rate is slightly changed with compressor speed. As compressor speed increases the mass flow rate increases. Figure (7) shows the pressure in condenser increases as compressor speed increases, while the pressure in the evaporator remains unchanged, this means that the compressor suction pressure is not a function of compressor speed. Figure (8) shows the refrigerant temperature at condenser inlet and saturation temperature. As compressor speed



increases the inlet refrigerant temperature increases, this due to increasing the refrigerant pressure, and then increasing the refrigerant enthalpy. The increase in the saturation temperature is due to the increase of refrigerant pressure.

Figure (9) shows the energy flow through the system. As compressor speed increases the energy flow increases, due to the increase in the work input to compressor. Figure (10) shows the system and cycle coefficient of performances, as compressor speed increases, the COP decreases. This is due to the increasing work input to compressor.

#### **Transient Response Due to a Sudden Change in Operation Conditions:**

Transient response due to a sudden change in operation conditions such as changing the compressor speed, expansion valve opening, and the changing of the water flow rate passing through the condenser and evaporator. For this purpose the software called "Thermosys Toolbox" was developed in AC&RC at the University of Illinois was used. The "Thermosys Toolbox" was used to model validation, analysis, and design[9]. This library was developed for use with MATLAB and its associated simulation program Simulink®.

#### **Complete Model Validation: Vapor compression Refrigeration**

For model validation, the complete system model is simulated in Matlab®. The component models for condenser, evaporator, expansion valve and compressor introduced earlier. For comparison of the model responses with the

experimental data, the model is fed with the component parameters and all the inputs applied to the experimental system are applied to the model too.

The output variables that are compared with the data are the refrigerant pressures in the evaporator and the condenser, refrigerant superheat at the evaporator outlet and the outlet water temperatures for the two heat exchangers. These variables are important for evaluating the system performance and efficiency, as well as for effective system design .

#### **Step Inputs to the Expansion Valve Opening:**

Input signal is applied to the expansion valve as shown in Figure (11) below. The response of the model to this input signal and the data are plotted in the following few figures. Here, the model is able to predict the dynamic characteristics of the data that can be seen, however the steady states are found to be quite off from the values measured in the data. The transient response for all the outputs is however met very closely by the model.

The model output and the experimental data can be compared in the following figures. The model behaves very close to the actual data in dynamic as well as steady state response as can be observed.

From the figures shown in this section, it can be inferred that the same model is able to predict the system response with a fair degree of accuracy for two different experimental data sets. There are some discrepancies in the steady state match however; all of the salient dynamic characteristics have

been captured by the model very well.

Model validation for the refrigeration systems is presented. The results show good agreement for different experimental data sets. Further, qualitative validation for receiver and accumulator models is also obtained. As the number of data sets used for validation increases, the confidence in the model also increases. It is clear from the results and graphs, that the evaporator is the most affected component with any changing in the operation parameters. Further, the choice of the model types showed a promising strategy for the dynamic modeling of the vapor compression refrigeration systems.

### Conclusions

The study is focusing mainly on physics based modeling of the vapor compression cycle and its components with the objectives of design prediction.

The results showed that the COP decreases as the compressor speed increases, in addition the time required to reach the steady state increases as well. The overall cycle models for single evaporator systems are further validated against different experimental data set, which indicated the possibility to confide in the models for accurate prediction of the cycle dynamics. These different models are combined with the existing Matlab® to form modular modeling surroundings for air conditioning systems.

The finite difference technique, lumped-parameters and the results presented in this investigation can be used for a variety of vapor

compression systems and dynamic problems. The comparison between the experimental and theoretical model exhibited a good agreement with an overall error about (5%).

It seems that the evaporator is the major component that affected by changing the operation conditions, and has the fastest response to any disturbance in operation conditions. It can be used as a controlled component in the vapor compression refrigeration systems.

### References

- [1] Lars, F. S. L., "Model Based Control of Refrigeration System"; Ph.D., thesis, Central R&C, Donfoss A/S, ISBN 87-90664-29-9, Nov., 2005.
- [2] MacArthur, J.W and Grald, E.W., "Prediction of Cyclic Heat Pump Performance with a Fully Distributed Model and a Comparison with Experimental Data", ASHRAE Transaction, part 2, Vol. 94, PP 1159-1178, 1988.
- [3] Sean, A. S., and Curt, O. P., "Semi-Theoretical Steady State and Transient Modeling of a Mobile Air Conditioning Evaporator". Paper No. ACRC-TR-37, University of Illinois, May, 1993.
- [4] Atear, O. E., Ileri, A., and Gogus, Y. "Transient Behavior of Finned Tube Cross-Flow Heat Exchangers", Int. J. Refrigeration, Vol. 18, PP 153-160, 1995.
- [5] James S., Miller, N.R., and Hrnjak, P., "A Sensor for Estimating the Liquid Mass Fraction of the Refrigerant Exiting an Evaporator" SAE Paper No. 2000-01-0976, 2000.

- [6] Xuquan, L., Chen, J., Chen, Z., Liu, W., Hu, W., and Liu, X., "A New Method for Controlling Refrigerant Flow in Automobile Air Conditioning" *Applied thermal Engineering*, Vol. 24, PP 1073-1085, 2004.
- [7] Xia, J., Winandy, E., Georges, B., and Lebrun, J., " Experimental Analysis of the Performances of Variable refrigerant Flow Systems", *Building Serv. Res. Technology*, Vol. 25, No. 1 PP 17-23, 2004.
- [8] Tarrad, A. H. and Shehhab, U. S., " The Prediction of Environment Effect on the Performance of a Vapor Compression Refrigeration System in Air Conditioning Application", *Engineering and Development Journal*, Vol. 11, No. 1, 2007.
- [9] Rasmussen, " Control-Oriented Modeling Of Transcritical Vapor Compression Systems" M.Sc, University of Illinois, 2002.
- [10] He, X., Liu, S., and Asada, " Modeling of Vapor Compression Cycles for Multivariable Feedback Control of HVAC System", *ASME J. Dynamic System Measurement and Control*, Vol. 119, pp. 183-191, 1997.
- [11] Deng, S., Misseenden, " Applying Classical Control theory for Validity and Simplifying a Dynamic Mathematical Model of an A/C Plant", *ASHRAE Transaction* Vol. 105 (part I), pp. 140-148,1999.
- [12] Wedekind, G.L., Stoecker, W.F., "Theoretical Model for Prediction of the Transient Response of the Mixture-Vapor Transition Point in Horizontal Evaporating Flow" *Heat Transfer J.*, No.2, PP 165-174, 1968.
- [13] Petti, N., Willatzen, M., Ploug-Sorensen, L., " A General Dynamic Simulation Model for Evaporators and Condensers in Refrigeration", Part I&II, *Int. J. of Refrigeration*, Vol. 21, No. 5, pp. 398-414, 1998.
- [14] Grald, E.W., Mac Arthur, J.W.," A Moving Boundary Formulation for Modeling Time-Dependent Two-Phase Flow", *Int. J. and Fluid Flow*, Vol. 13 No. 3, pp. 266-272, 1992.
- [15] Yasuda, H., Machielsen, C.H.M. and Touber, S. "Simulation of Transient Behavior of a Compression-Expansion Refrigeration System" *IIR Commission B2, C2*, PP 147-154, 1979.
- [16] Bendapndi, S., Brann, J. E., " A Review of Literature on Dynamic Model of vapor Compression Equipment", *ASHRAE Report # 4036-5*, May 2002.
- [17] Mithrorathe, P., Wijeeysundera, N.E., " An Experimental and Numerical Study of the Dynamic Behavior of Counter Flow Evaporator", *Int. J. of Refrigeration*, Vol. 24, pp. 554-565, 2001.
- [18] Streeter, V. L., and Wylie, E. B., "Fluid Mechanics", 7th McGraw-Hill, Tokyo, Japan, 1979.
- [19] Xiang-Dong, H., Sheng L. , Asada, H.H. and, Itoh, H., "Multivariable Control of Vapor Compression Systems", *HVAC&R Research*, Vol. 4, No. 3, 1998.

- [20] "Product Description", Hoke, [www.hoke.com](http://www.hoke.com), 2002.
- [21] Stearn, R. F., Johnson, R.R., Jackson, R. M., Larson, C. A., " Flow Measurement with Orifice Meters", D. Van Nostrand Company, Toronto, 1951.
- [22] Abdullah, M. N. " Transient Response Of Subcritical Vapor Compression Refrigeration System" Ph.D. thesis, University of Al-Mustansiriya , College of Engineering, 2008.

**Nomenclature:**

Variable	Definition	Units
A	Area	(m <sup>2</sup> )
Cv	Coefficient of Discharge	----
D	Pipe Diameter	(m)
H	Enthalpy	(kJ)
L	Length	(m)
p	Perimeter	(m)
P	Pressure	N/m <sup>2</sup>
Q	Heat Transfer	(w)
Red	Reynolds Number	----
S	Entropy	(KJ)
T	Temperature	C <sup>0</sup>
U	Internal Energy	(kJ)
Cp C <sup>0</sup> )	Heat Capacity	(kJ/kg
h	Specific Enthalpy	(kJ/kg)
m	Refrigerant mass	(kg)
t	Time	sec
u	Specific Internal Energy	(kJ/kg)
z	Length Dimension	m
<b><u>Creek Symbols</u></b>		
α C <sup>0</sup> )	Heat Transfer Coefficient	(W/m <sup>2</sup>
γ	Mean Void Fraction	----
ρ	Density	kg/m <sup>3</sup>
μ	Viscosity	Pa.s
<b><u>Subscript</u></b>		
l	<b><u>Definition</u></b> Liquid Refrigerant	
g	Vapor Refrigerant	
o	Outlet	

---

1,2,3	Regions of Heat Exchange
i	Inlet
int	Interface
is	isentropic
r	Refrigerant
rev	Reversible
w	Wall
wa	Water

**Abbreviations:**

A/C	Air Conditioning
AC&RC	Air Conditioning and Refrigeration Center
COP	coefficient of Performance
EEV	Electronic Expansion Valve
GPM	Gallon Per Minute
ODE	Ordinary Differential Equations
PDE	Partial Differential Equation
TXV	Thermostatic Expansion Valve
R-12	Refrigerant CCl <sub>2</sub> F <sub>2</sub>
VC	Vapor Compression
VRF	Variable refrigerant flow

Table (1) The Cooling Unit Physical Specifications

Component	Parameter	Unit	Value	Comment
Evaporator	Heat Exchanger Type		counterflow	Manuf. Data Sheet
	Material		Copper	Manuf. Data Sheet
	Specific Heat	kJ/kg.K	0.383	Material Standards
	Mass	kg	2.641	Manuf. Data Sheet
	Internal Volume	Cu.m	4.7885E-4	Calculated
	External Surface Area	Sq.m	0.24338	Calculated
	Cross Sectional Area	Sq. m	78.5E-6	Calculated
	Internal Surface Area	Sq. m	0.19154	Calculated
	Total Length of Fluid Flow	m	6.1	Manuf. Data Sheet
	Hydraulic Diameter	m	0.0127	Manuf. Data Sheet
	Two Phase Flow Heat Transfer Coefficient	kW/sq.m/K	2	Tuned Parameter
	Superheat Flow Heat Transfer Coefficient	kW/sq.m/K	0.2402	Calculated
	External Fluid Heat Transfer Coefficient	kW/sq.m/K	0.405	Calculated
	Slip Ratio		2	Tuned Parameter
External Fluid Specific Heat	kJ/kg.K	4.18	Material Standards	
Condenser	Heat Exchanger Type		counterflow	Manuf. Data Sheet
	Material		Copper	Manuf. Data Sheet
	Specific Heat	kJ/kg.K	0.383	Material Standards
	Mass	kg	5.0748	Manuf. Data Sheet
	Internal Volume	Cu.m	9.2475E-4	Calculated
	External Surface Area	Sq.m	0.4697	Calculated
	Cross Sectional Area	Sq. m	78.5E-6	Calculated
	Internal Surface Area	Sq. m	0.3698	Calculated
	Total Length of Fluid Flow	m	11.78	Manuf. Data Sheet
	Hydraulic Diameter	m	0.0127	Manuf. Data Sheet
	Two Phase Flow Heat Transfer Coefficient	kW/sq.m/K	2	Tuned Parameter
	Superheat Flow Heat Transfer Coefficient	kW/sq.m/K	1.423	Calculated
	Subcooled Flow Heat Transfer Coefficient	kW/sq.m/K	1.427	Calculated
	External Fluid Heat Transfer Coefficient	kW/sq.m/K	0.521	Calculated
Slip Ratio		2	Tuned Parameter	
External Fluid Specific Heat	kJ/kg.K	4.18	Material Standards	
Receiver	Internal Volume	Cu. m	0.00029	Manuf. Data Sheet
	UA Value of Receiver	kWK	0	Full Insulation Assumed
Expansion Valve	Expansion Base Area	Sq. m	1E-6	Manuf. Data Sheet
	Empirical Parameter Dv		0.6	Calculated
	Empirical Parameter Ev		0.1	Calculated
	Empirical Parameter n		0.5	Calculated
	Rate Limit		1	Calculated
Compressor	Compressor Displacement	Cu. m	100E-6	Manuf. Data Sheet
	Empirical Parameter Ck		0.988	Calculated
	Empirical Parameter Dk		0.1681	Calculated
	Empirical Parameter n		1.4	Calculated
	Empirical Parameter Ak		-0.0357	Calculated
	Empirical Parameter Bk		0.9227	Calculated
	Rate Limit		50	Calculated

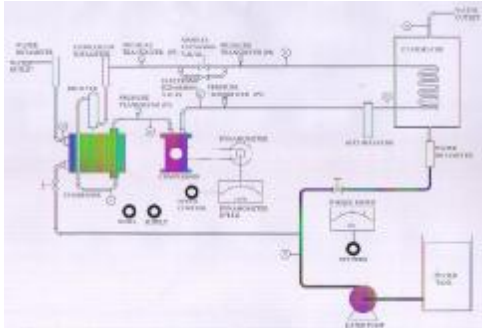


Figure (1) A Schematic Diagram of Test Rig



Figure (2) A Photograph for Test Rig



Figure (3) Test Rig (rear side)

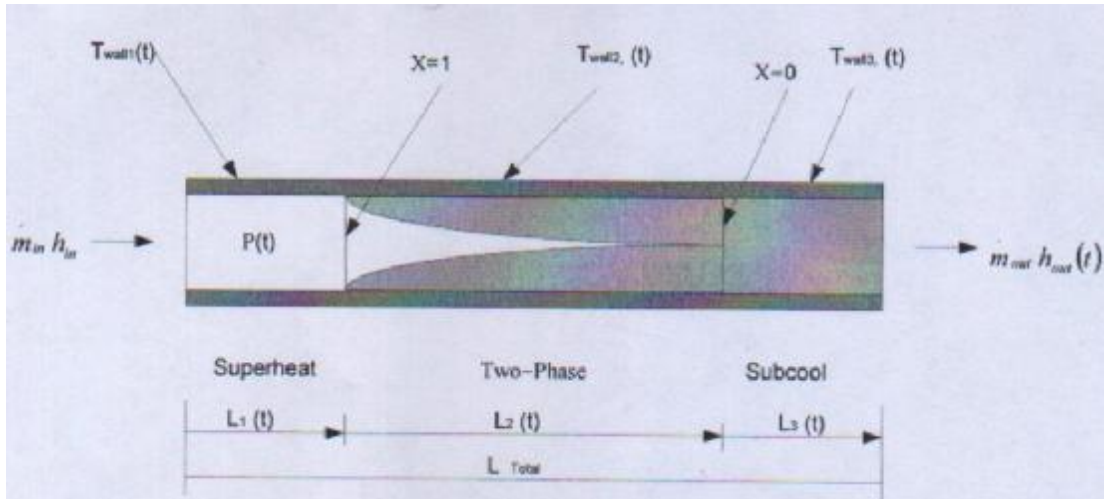


Figure (4) Three Region Condenser [9]

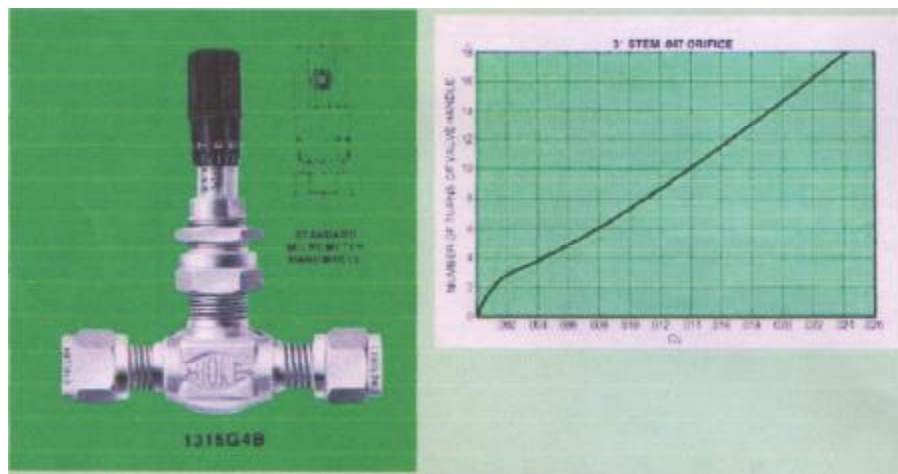


Figure (5) Valve with Coefficient of Discharge Characteristics [20]



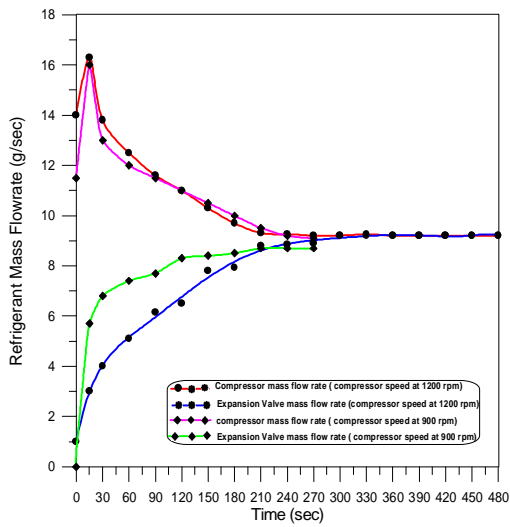


Figure (6) Compressor and Expansion Valve Mass Flow Rate Response

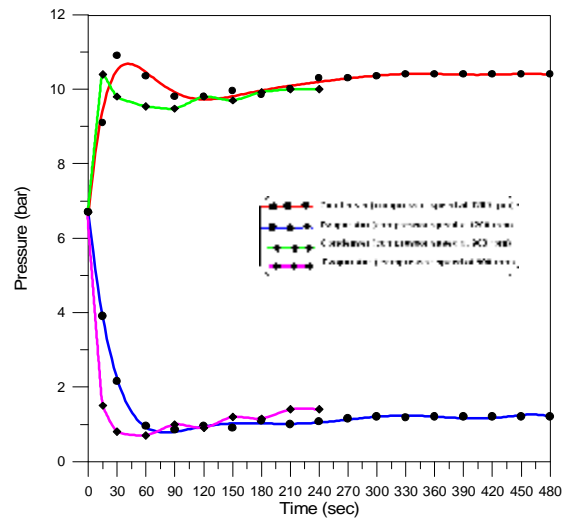


Figure (7) Condenser and Evaporator Pressure Response (Start-up)

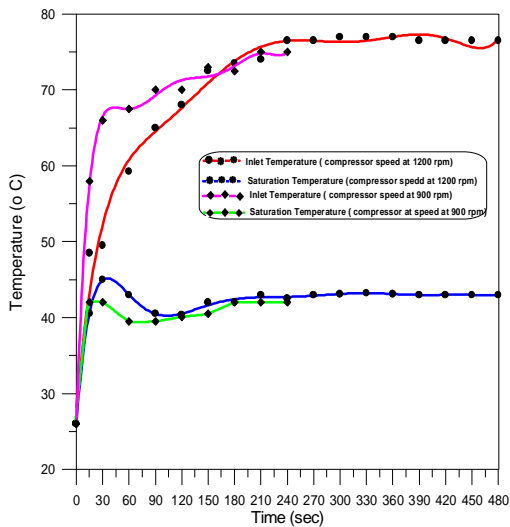


Figure (8) Condenser Inlet and Saturated Temperature Response

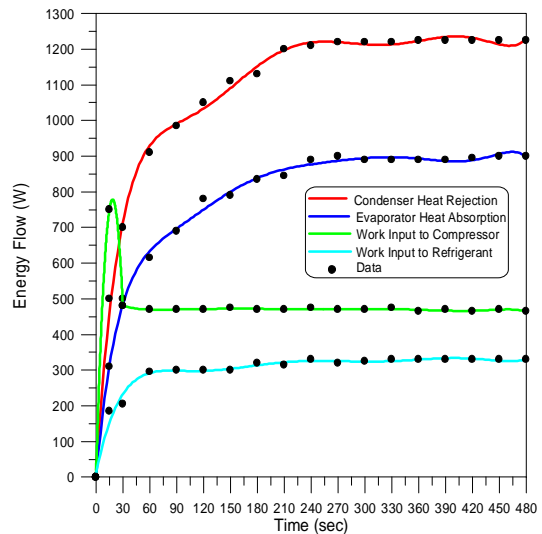


Figure (9) Energy System Response

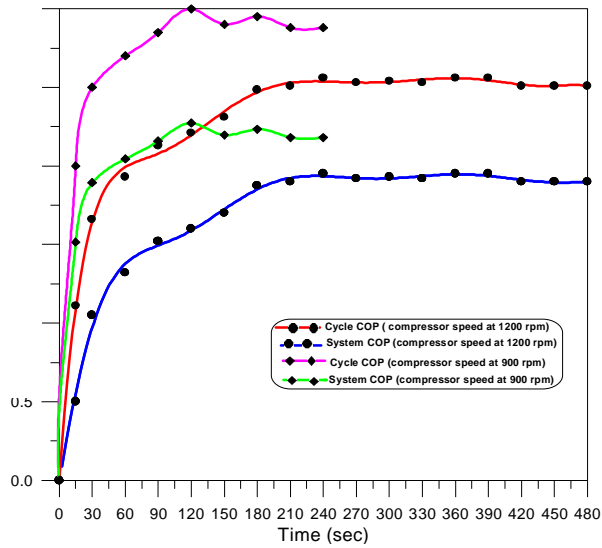


Figure (10) Response of Coefficient of Performance.

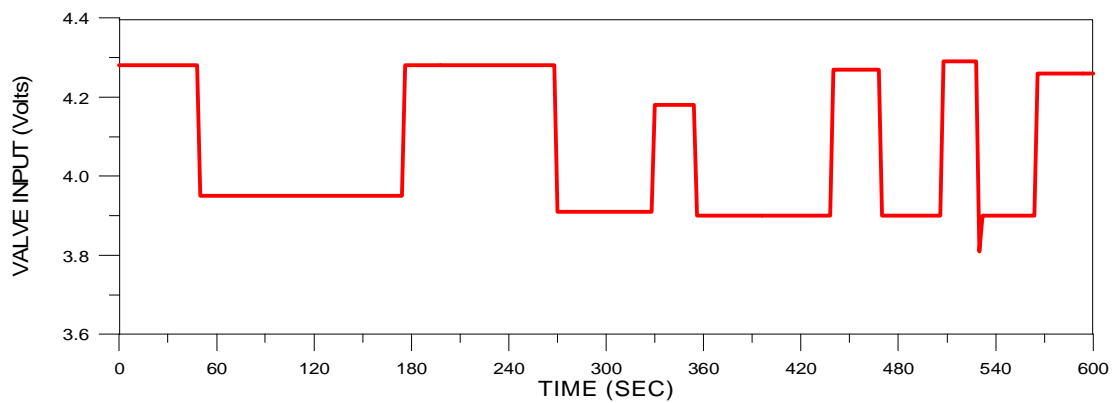


Figure (11) Step Input to the Expansion Valve

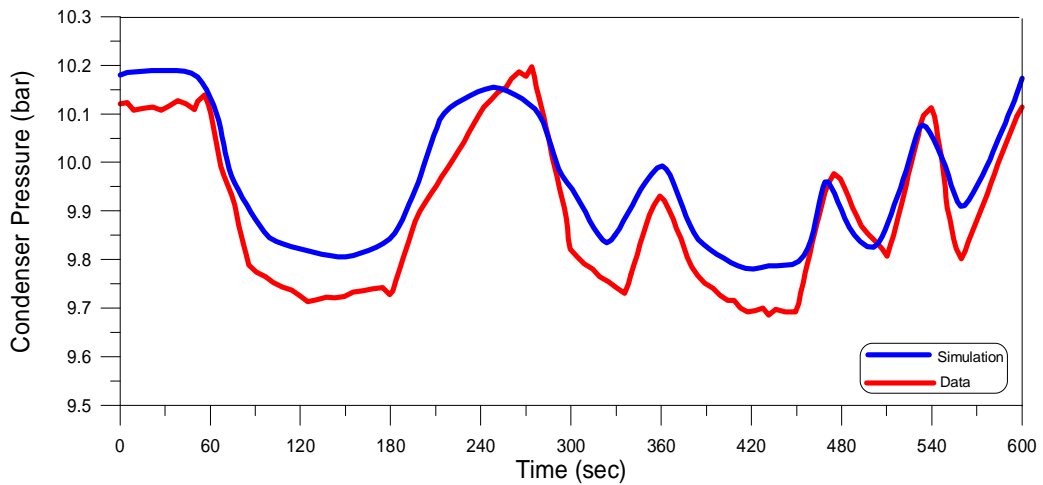


Figure (12) Refrigerant Pressure at the Condenser

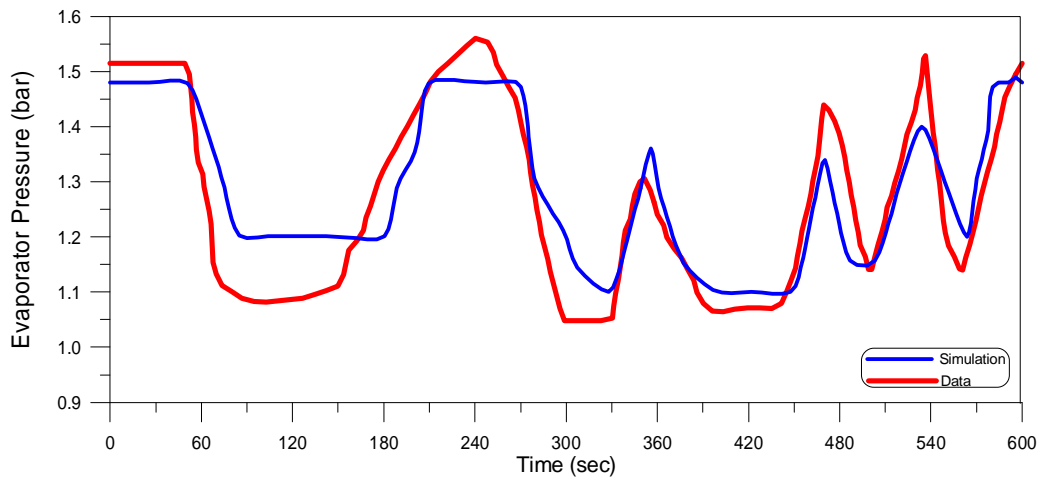


Figure (13) Refrigerant Pressure at Evaporator

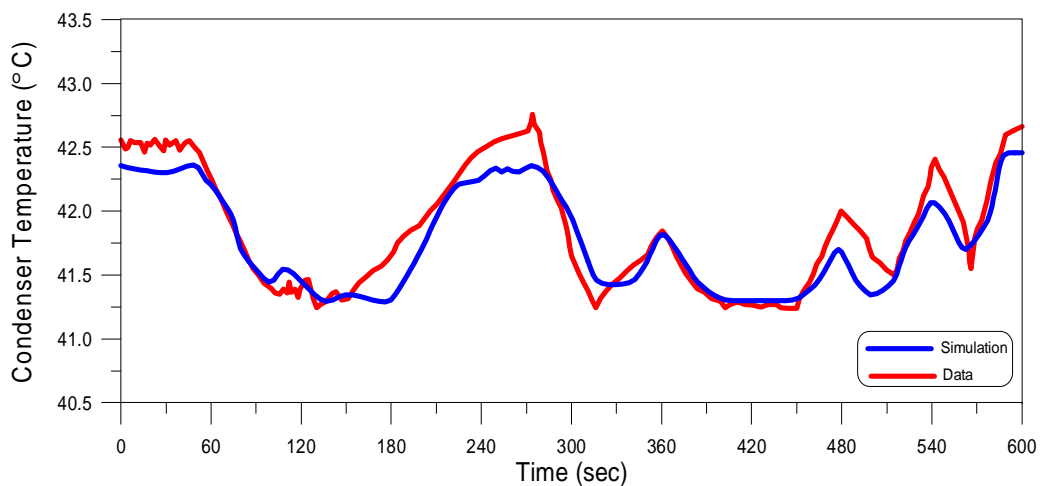


Figure (14) Refrigerant Temperature at the Condenser

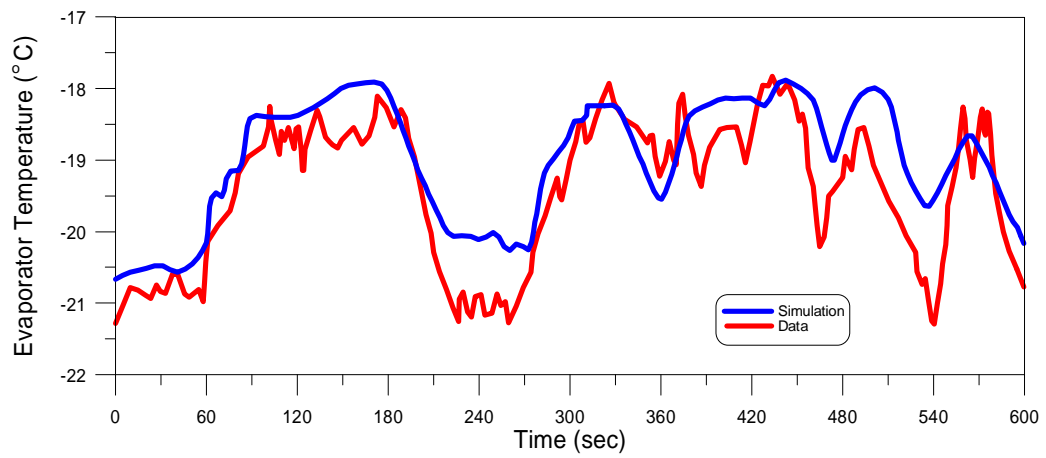


Figure (15) Refrigerant Temperature at the Evaporator

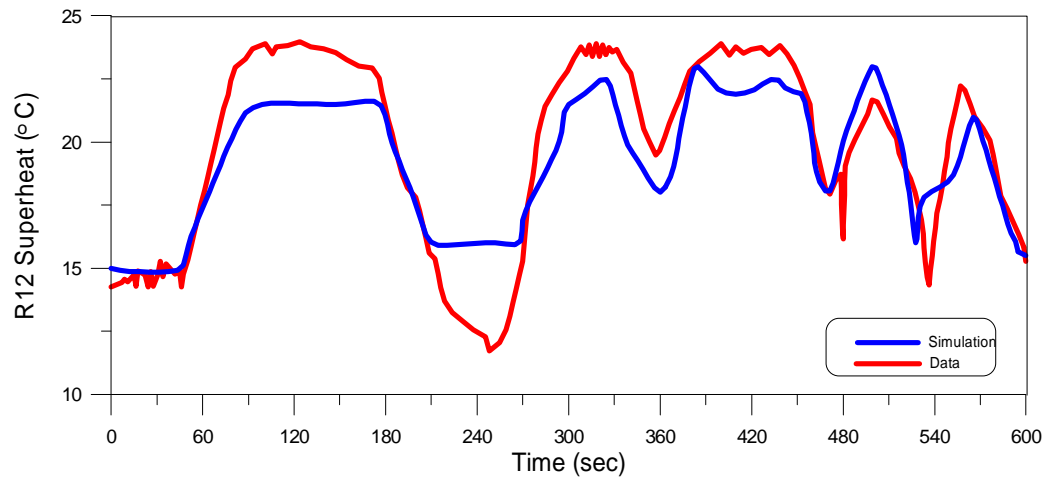


Figure (16) Refrigerant Superheat at the Evaporator Outlet